

INTERACTION OF MEMBRANE STRESSES AND MAGMA ASCENT AT LARGE IMPACT BASINS ON MARS AND MERCURY. P. J. McGovern¹ and T. R. Watters², ¹Lunar and Planetary Institute, Universities Space Research Association, 3600 Bay Area Blvd., Houston TX 77058, USA (mcgovern@lpi.usra.edu), ²CEPS, Smithsonian Institution, Washington, DC 20560-0315 (watterst@si.edu).

Introduction: Impact basins are among the most striking structures on planetary surfaces. Impacts excavate substantial amounts of crustal material, resulting in lateral and upward displacement of both crustal and mantle material. This movement, along with magma emplacement, can result in loading of the surrounding lithosphere, with implications for the stress state. Stresses, in turn, influence subsequent magmatic emplacement modes. Here, we use a simple mathematical model of the broad-scale loading effects induced by basins to investigate how such loading may control magmatism within and around the basins.

Method: By the term “basin”, we mean an impact structure of substantial diameter relative to the circumference of the planet (see Table 1). Such loads are supported dominantly by a “membrane”, or stretching, response of the lithosphere [e.g., 1], with stresses that are constant with depth. This stress state can be interpreted via the criterion of Anderson [2]: magma tends to move in intrusions that form perpendicular to the least compressive principal stress. Thus, models with at least one horizontal normal stress in extension favor magma ascent in dikes, whereas models with both horizontal normal stresses compressive will inhibit ascent. Note that flexural (plate bending) stresses are important for narrower loads; they vary with depth, requiring an additional magma ascent criterion [3-4].

We use an elastic spherical shell solution in the membrane stress limit with a Gaussian load [1] to illustrate the effects of broad-scale basin loading states on lithospheric stresses. We assume that the baseline post-impact-adjustment compensation state is Airy isostasy, neglecting stresses from crustal thickness gradients [5-7]. We then explore departures from isostasy, expressed as upward or downward loads. Loads that could cause a net downward deflection of the lithosphere include an initial super-isostatic state [e.g., 8], dense intrusions, or surface loads [e.g., 9], whereas uplift-inducing loads include an sub-isostatic initial adjustment, upward mantle flow in response to melt or thermal perturbations [10], or lateral crustal flow [6-7].

Results: *Downward load:* The radial stress is compressional everywhere (Fig. 1a). The circumferential stress passes from central compression to distal extension at $r_{\text{trans}} \approx 0.55 r_0$, with a peak at $r_{\text{peak}} \approx 0.9 r_0$. The intrusion ascent criterion predicts a shutoff at the center of the basin (effect is strongest at center, decreasing with increasing r). Beyond r_{trans} , ascent is possible in conduits perpendicular to extensional hoop stress: radial dikes, possibly expressed at the surface as radial

graben. Note that a purely tectonic interpretation [2] predicts strike-slip faulting outward of r_{trans} , at least above the depth where the lithostatic stress becomes more compressional than the radial stress.

Upward load: This is the reflection about the x-axis of the downward load case in Fig. 1a. The radial stress is extensional everywhere, and strongest at the center. The circumferential stress transitions from extensional to compressional at $r_{\text{trans}} \approx 0.55 r_0$. The ascent criterion predicts that central magma ascent is greatly favored. There is no preferred dike orientation near the center, but an increasing preference for circumferential dikes/graben with increasing r , and solely circumferential beyond r_{trans} . The tectonic faulting prediction beyond r_{trans} is the same as above, but with the circumferential stress controlling the transition depth.

Mars: Borealis: For the proposed Borealis basin [11-12], Tharsis is located just beyond the peak circumferential stress area. Further, the trends of Ceraunius and Tractus Fossae (“CT”) graben systems between Alba Patera and central Tharsis lie roughly radial to Borealis, consistent with a downward-load, membrane stress-driven, intrusive origin. Thus, Tharsis and the CT trend were likely favored zones for magma ascent on the rim of Borealis, but basin loading alone cannot explain why volcanism was concentrated at one particular azimuth. Mantle convection models suggest that upwellings can be nucleated near steps in surface structure [13], accounting for the position of Tharsis along the crustal dichotomy boundary. Such an upwelling may have been influenced by the ease of magma ascent at the rim of Borealis. The upwelling would localize in axisymmetric geometry, exploiting the favorable stress state on the rim at a particular point to produce an immense volcanic complex. Thus, a Borealis impact may have contributed to the rise of Tharsis in two ways, by “preparing” both the mantle (for a large plume) and the lithosphere (for magma ascent).

There are also indications of an upward load at Borealis. As the CT trend bends around Alba Patera, becoming Alba and Tantalus Fossae (“AT”), the graben deflect to the northeast. When projected about the proposed center of Borealis [12], this deflection is seen to be roughly circumferential to the basin, at a value of r where circumferential graben are predicted by both the intrusive and tectonic criteria. The graben of Elysium Fossae, and Mareotis and Tempe Fossae (“MT”) in Tempe Terra, also follow a circumferential trend, but at somewhat greater r . We suggest that the initial load direction at Borealis was upward, producing stresses

that influenced the AT, Elysium, and MT trends and facilitated volcanic infilling near the center. The infilling subsequently caused the loading polarity to change to downward, producing the stress state that favored growth of Tharsis and the CT graben.

Hellas: Several large volcanoes ring the rim of Hellas. Hadriaca, Peneus, and Amphitrites Paterae are all located near the predicted peak extensional stress zone (Fig. 1), suggesting that they are associated with radial intrusions. Analysis of gravity/topography admittances suggests the presence of a limited Hellas mascon [14], a finding consistent with the downward load scenario. The limited nature of the rim volcanism is in accord with the small magnitude of the mascon load. This scenario is also consistent with proposed intense volcanism-induced erosion in the western Hellas rim [15] and an intrusive origin for the (subsequently eroded) radial Dao and Harmahkis Valles.

Utopia: This basin is mostly filled, probably by high-density volcanics [16]. Perhaps an initial upward load similar to that proposed for Borealis above led to rapid infill. However, producing so much infill before the loading polarity changes would be difficult. More likely, voluminous material from outside basin is flowing in, in accord relatively young age of surface materials at Utopia. Our results suggest a variation on this idea: much of the infill may come from vents in the high-stress inner rim area: flows from such vents would naturally flow in to the basin, increasing the central load and thus the radial stresses, making rim magma ascent even more favorable (a self-reinforcing scenario). The difference in crustal thickness between the Utopia and Hellas impact sites may in part account for the stark difference in infill: mantle melts have less distance to ascend in the former case.

Mercury: Imaging from the first MESSENGER flyby of Mercury [17-18] revealed evidence for a large volcanic complex and rimless depressions surrounded by pyroclastic deposits near the rim of the Caloris basin. Its position is very close to that of the peak extensional membrane stress predicted by the downward load model, and its elongation in a radial direction [18] is consistent with the predicted orientations of dikes in that model. Plains volcanism external to Caloris, sometimes implicated in loading scenarios [19-20], is broadly consistent with the distal extensional stress states predicted by either downward or upward loading membrane stress scenarios. In principle, the scenarios could be distinguished if feeder dike-related extensional features in the circum-Caloris plains could be found and their orientations with respect to Caloris classified (none have been detected to date).

We predict that a modest mascon will be found at Caloris. Several predictions of a substantial Caloris mascon have been made based on mechanical loading scenarios [e.g., 20-21]. Given that only one Caloris rim

volcanic complex has been found, a Caloris mascon may be more modest than previously predicted, comparable to the weak Hellas mascon. Alternatively, the mantle beneath Caloris was less magmatically fertile than that beneath Utopia or even Hellas.

Table 1: Large impact basin diameters and fractions of planetary circumference.

Basin	Diameter [km]	$D/(2\pi R_{\text{planet}})$, %
Borealis (Mars)	9550 ± 1000 [12]	40 - 49
Utopia (Mars)	2350 ± 350	9.3 - 13
Hellas (Mars)	2120 ± 300 [12]	8.5 - 11
Caloris (Mercury)	1550 ± 200 [17]	8.7 - 10

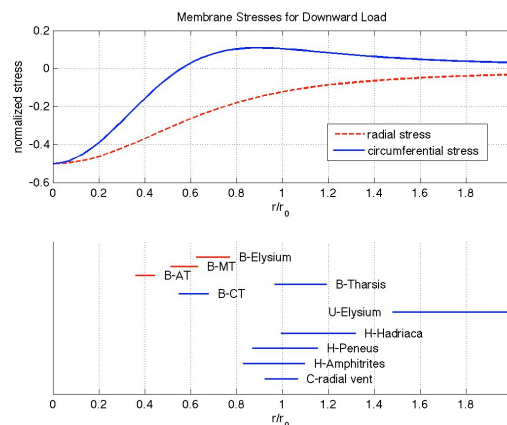


Fig. 1. (a) Non-dimensional plot of membrane stress versus normalized radius for a downward load on the lithosphere [1]; radial stress in red dashed line, circumferential stress in blue solid line. (b) Normalized radial positions of volcanic or tectonic structures with respect to basins Caloris (C), Hellas (H), Utopia (U), and Borealis (B). Blue lines for features interpreted by downward loads, red for upward.

References: [1] Turcotte D. L. et al. (1981), *JGR*, 86, 3951. [2] Anderson E. M. (1951), *The Dynamics of Faulting and Dyke Formation with Applications to Britain*, Oliver and Boyd, Edinburgh, 206pp. [3] Rumpf M. E. and McGovern P. J. (2007), *LPS XVIII*, Abstract #1374. [4] Litherland M. and McGovern P. J. (2009), *LPS XL* (this volume). [5] Banerdt W. B. (1986), *JGR*, 91, 403. [6] Nimmo F. and Stevenson D. J. (2001), *JGR*, 106, 5085. [7] Watters et al. *Geology*, 33, 669, 2005. [8] Neumann G. A. et al. (1996), *JGR*, 101, 16,841. [9] Solomon S. C. and Head J. W. (1980), *Rev. Geophys. Space Phys.*, 18, 107. [10] Elkins-Tanton L. T. et al. (2004), *EPSL*, 222, 17. [11] Wilhelms D. E. and Squyres S. W. (1984), *Nature*, 309, 138. [12] Andrews-Hanna J. C. et al. (2008), *Nature*, 453, 1212. [13] King S. D. (2006), *AGU Fall Meeting Abstract* #P31B-0144. [14] P. J. McGovern et al. (2002), *JGR*, 107, doi:10.1029/2002JE001854. [15] Tanaka et al. (2002), *GRL*, 29, doi:10.1029/2001GL013885. [16] Searls M. L. et al. (2006), *JGR*, 111, doi:10.1029/2005JE002666. [17] Murchie S. L. et al. (2008), *Science*, 321, 73. [18] Head J. W. et al. (2008), *Science*, 321, 69. [19] Melosh H. J. and McKinnon W. B. (1988), in *Mercury*, U. of Arizona Press, Tucson, 374. [20] Kennedy P. J. et al. (2008), *JGR*, 113, doi:10.1029/2007JE002992. [21] Matsuyama I. and Nimmo F. (2009), *JGR*, in press.